Stability Analysis of Bay Bridge Saddle Configuration

Sanjay Govindjee[1]

Abstract: In this brief note, we present the results of a full finite deformation analysis of a system similar to the Oakland-San Francisco Bay Bridge saddle repair system. The dimensions used are for illustration purposes but are intended to be in the range of those associated with the real system. The saddle system is seen to be unstable as designed. With a small modification the system can be made stable (self-centering).

DOI: 10.1061/(ASCE)ST.1943-541X.0000245

CE Database subject headings: Rehabilitation; Bridges; California; Structural analysis; Deformation.

Author keywords: Saddle repair; Stability; Oakland-San Francisco Bay Bridge.

System

A schematic of a system geometrically similar to the Oakland-San Francisco Bay Bridge saddle repair system is shown in Fig. 1 (left) and Fig. 2 (left). This basic system was used to repair a cracked eyebar on the bridge in early September 2009. In mid-October 2009, the repair system failed in a dramatic fashion. It was reinstalled with some modifications at the end of October 2009 but still retained the basic characteristics shown. In December 2009, it was removed after the installation of a new eyebar.

The repair system consists of two saddle pieces that cup to the upper and lower pins holding the eyebars. The saddles are pulled together by four prestressed bars (two used in this simplified two-dimensional analysis). This system was intended to take up the load previously held by a damaged eyebar—one of four eyebars in total between the two pins. In this analysis, the prestressed bars are assumed to be connected to the saddles by frictionless pivots. The primary degrees of freedom for the system are the rotations of the top and bottom saddles, θ_1 and θ_2, respectively. Each saddle can rotate independent of the other. With rotation, the attachment points for the bars move resulting in changes in strain in the bars. A proper analysis of this system requires the consideration of finite deformation kinematics since higher than second-order kinematics are needed to make a definitive statement on the system's stability. Shown in Fig. 1 (right) and Fig. 2 (right) is an alternative configuration where the attachment points for the prestressed bars are inside the main pins. This configuration is also analyzed.

System Potential Energy

The potential energy of the system consists of the stored elastic energy in the two bars

$$\Pi(\theta_1,\theta_2) = \frac{1}{2}k\Delta_1^2(\theta_1,\theta_2) + \frac{1}{2}k\Delta_2^2(\theta_1,\theta_2) \tag{1}$$

where k=stiffness of the bars and Δ_i=length changes from their reference unstressed lengths L_i^o. The Δ_i depend on the prestressing and the rotations θ_1 and θ_2. In our evaluation we account for the bars going slack by setting the energy contribution to zero when the distance between the attachment points falls below the unstressed lengths. In our examples we have assumed a prestressing of 200 $\mathrm{N/mm^2}$ (equivalent to a 1 millistrain prestrain). The prestrain displacement $\delta_i = L_i^o \epsilon_{\mathrm{pre}}$ and thus

$$\Delta_i = \delta_i + \left\| [\boldsymbol{R}(\theta_1)\boldsymbol{x}_i^{\mathrm{top}} + \boldsymbol{x}^{\mathrm{pp}}] - \boldsymbol{R}(\theta_2)\boldsymbol{x}_i^{\mathrm{bottom}} \right\| - L_i^o \tag{2}$$

where $\boldsymbol{x}_i^{\mathrm{top}}$=vector from the center of the upper main pin to the top attachment point of the bar; $\boldsymbol{x}_i^{\mathrm{bottom}}$=vector from the center of the lower main pin to the bottom attachment point of the bar; and $\boldsymbol{x}^{\mathrm{pp}}$=vector from the center of the lower main pin to the center of the upper main pin. The rotations

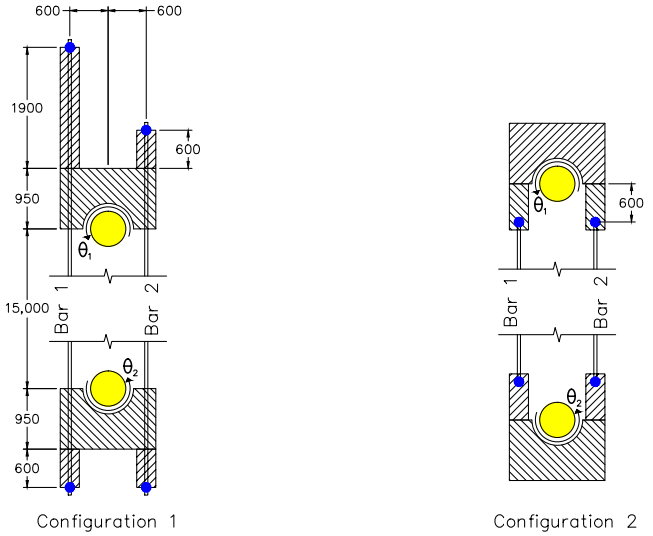

Fig. 1. Configurations analyzed: (Left) Bar attachments above the main pins. (Right) Bar attachments between the main pins. Bars are assumed to be attached with pin joints (shown as dark dots). Assumed dimensions are given for illustrative purposes (actual values differ).

[1]Professor, Structural Engineering, Mechanics, and Materials, Dept. of Civil Engineering, Univ. of California, Berkeley, Berkeley, CA 94720. E-mail: s_g@berkeley.edu

Note. This manuscript was submitted on December 2, 2009; approved on May 22, 2010; published online on May 28, 2010. Discussion period open until May 1, 2011; separate discussions must be submitted for individual papers. This technical note is part of the ***Journal of Structural Engineering***, Vol. 136, No. 12, December 1, 2010. ©ASCE, ISSN 0733-9445/2010/12-1613–1618/$25.00.

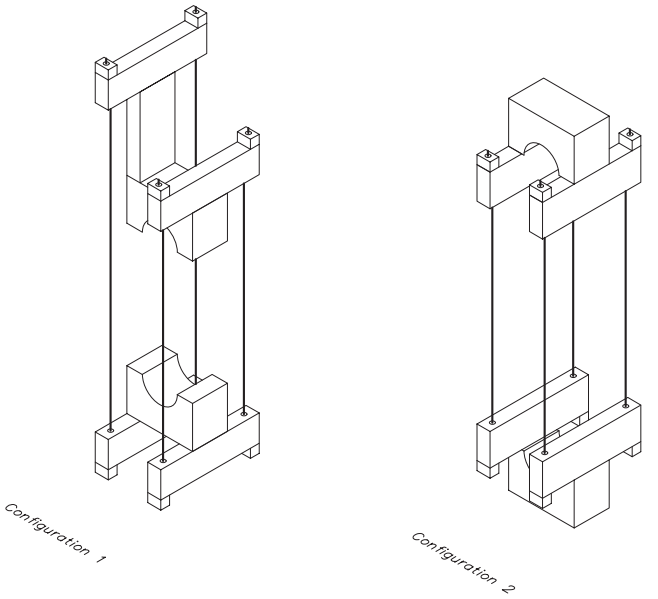

Fig. 2. Isometric view of two configurations: (Left) Configuration 1 similar to the as built system. (Right) Configuration 2 alternative configuration (not to scale).

$$\boldsymbol{R}(\theta_i) = \begin{bmatrix} \cos(\theta_i) & -\sin(\theta_i) \\ \sin(\theta_i) & \cos(\theta_i) \end{bmatrix} \tag{3}$$

and account for full finite rotations which are important when considering the kinematics of the system when the saddles corotate. Stability of the system can be assessed by an examination of the structure of the potential energy at equilibria with respect to kinematic variations. Equilibria occur at stationary points, and convexity at a stationary point indicates stability, whereas concavity or a saddle structure indicates an instability; see, e.g., classical texts such as Timoshenko and Gere (1961) or Fung (1965).

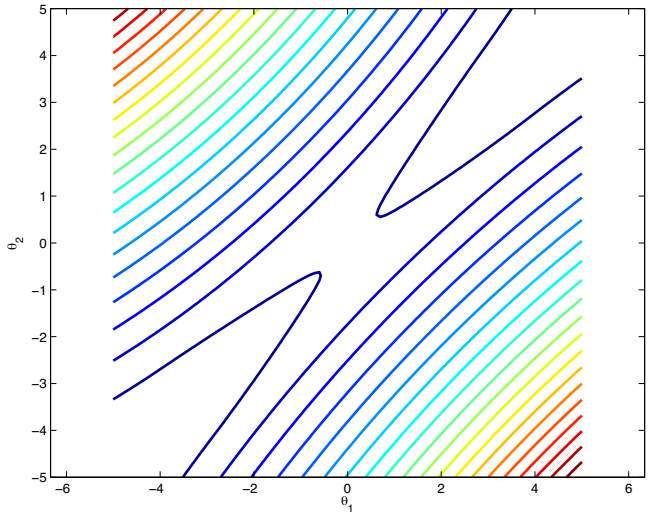

Fig. 3. Potential energy contour lines as a function of the saddle rotations for Configuration 1. An equilibrium is visible at zero total rotation, but it possesses an unstable saddle-point structure. Contour values increase to the upper left and lower right.

Configuration 1: Installed Configuration

Shown in Fig. 3 is the potential energy of the system with respect

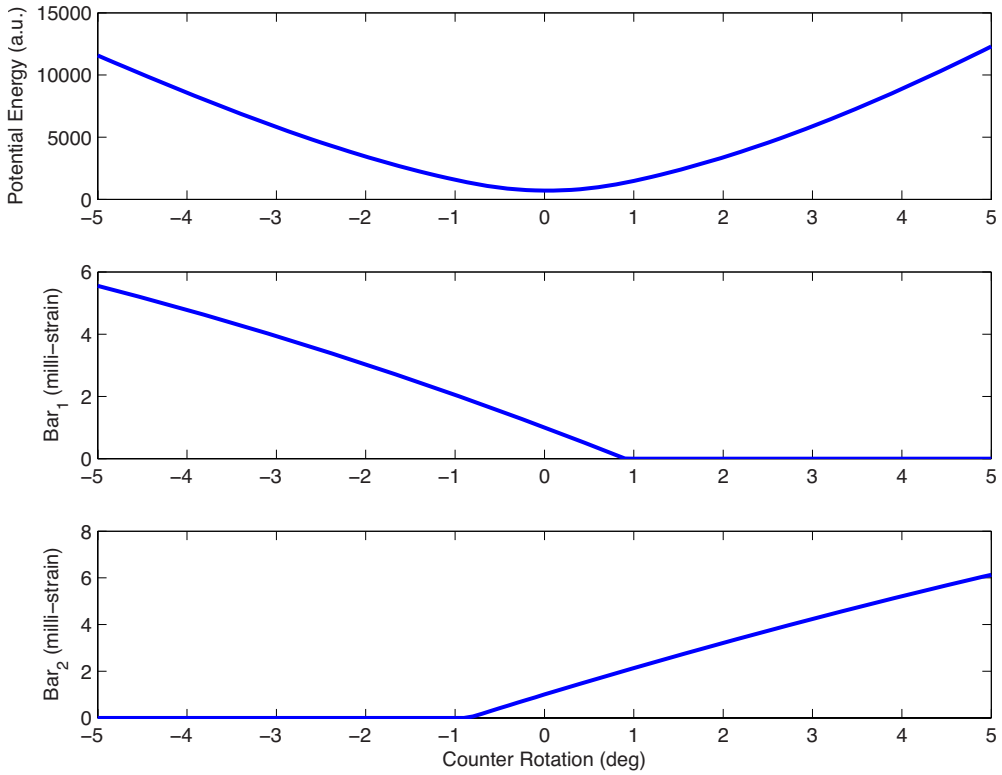

Fig. 4. Configuration 1 behavior for counter-rotating saddles ($\theta_1 = -\theta_2$). (Top) Potential energy is seen to be stable. (Middle) Strain in Bar 1. (Bottom) Strain in Bar 2. Strains are zero when the bars go slack.

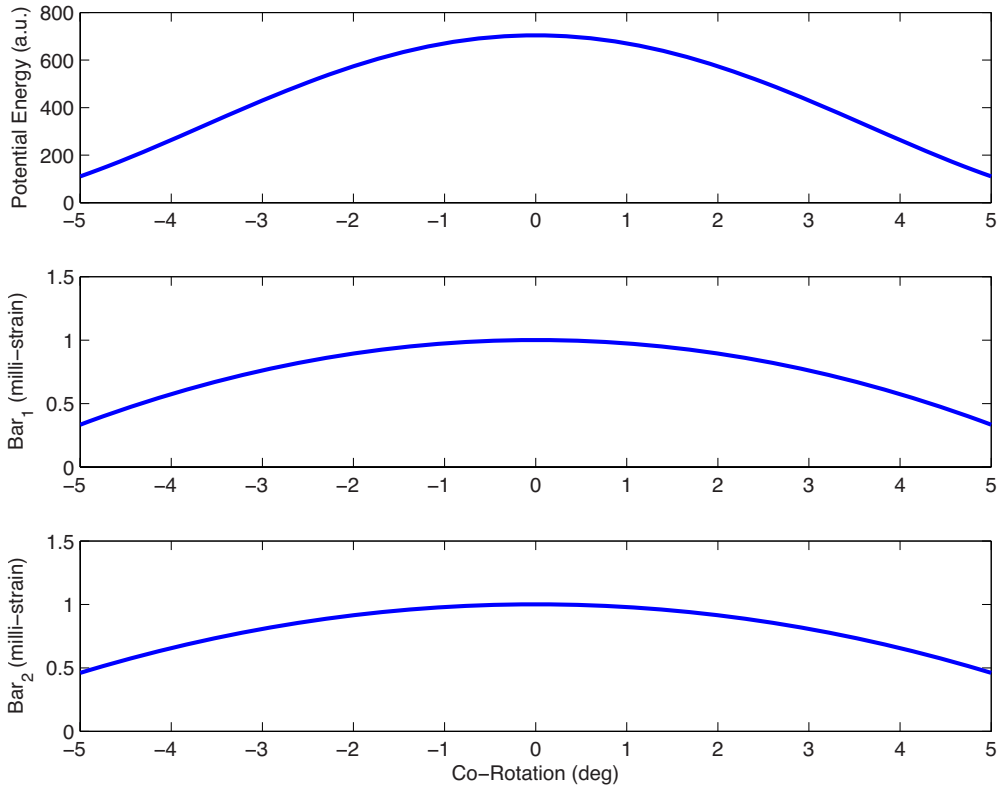

Fig. 5. Configuration 1 behavior for corotating saddles ($\theta_1 = \theta_2$). (Top) Potential energy is seen to be unstable. (Middle) Strain in Bar 1. (Bottom) Strain in Bar 2.

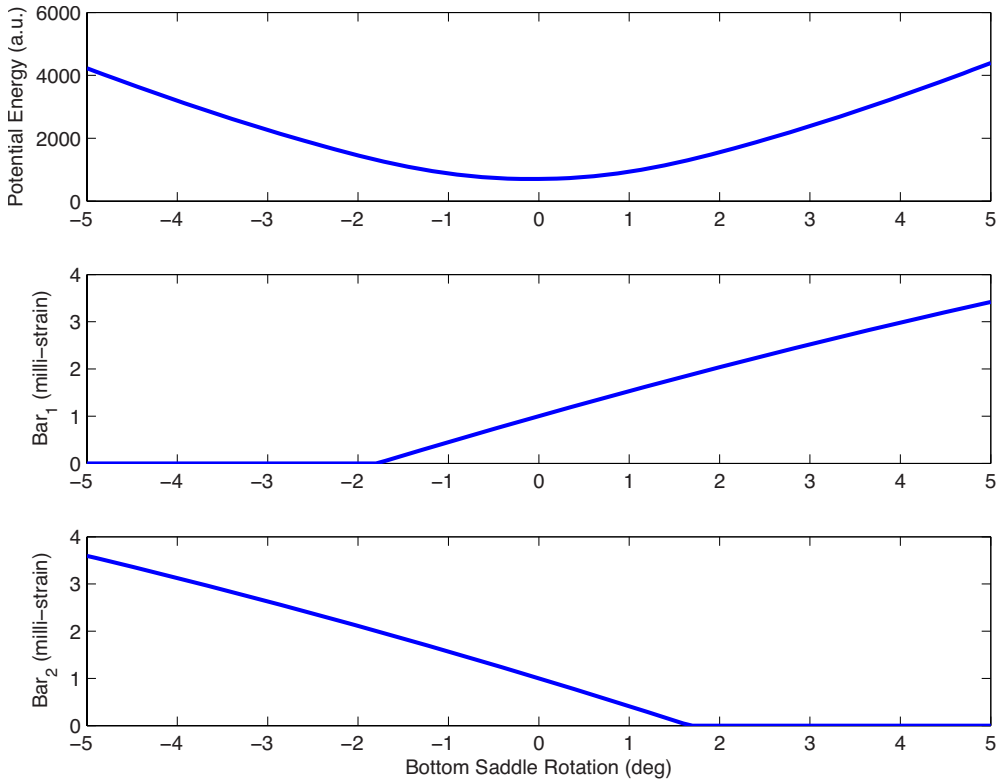

Fig. 6. Configuration 1 behavior with top saddle fixed ($\theta_1 = 0$; θ_2 free). (Top) Potential energy is seen to be stable. (Middle) Strain in Bar 1. (Bottom) Strain in Bar 2. Strains are zero when the bars go slack.

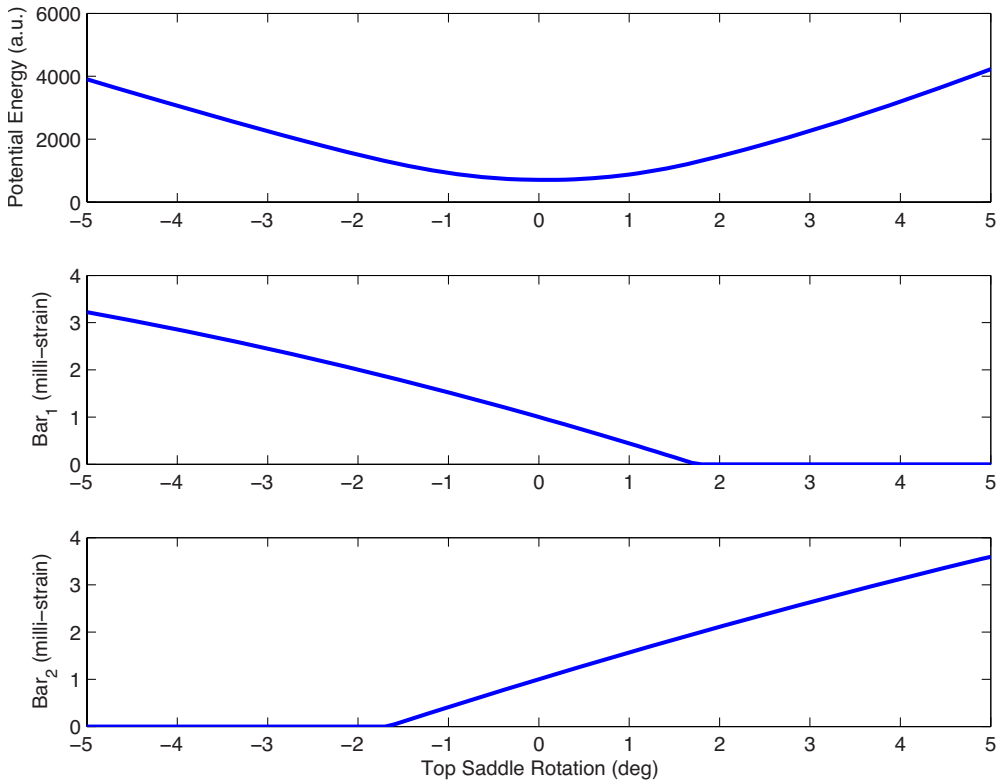

Fig. 7. Configuration 1 behavior with bottom saddle fixed (θ_1 free; $\theta_2=0$). (Top) Potential energy is seen to be stable. (Middle) Strain in Bar 1. (Bottom) Strain in Bar 2. Strains are zero when the bars go slack.

to the saddle rotations. When the saddles counter-rotate the energy grows and the system is seen to be stable against this type of motion. A section cut of the energy surface for $\theta_1=-\theta_2$ is shown in Fig. 4 (top) to emphasize this point. Also shown in Fig. 4 (middle and bottom) are the strains in the bars along this path. Depending on the direction of rotation one bar unloads and the other loads. With excessive rotations individual bars can go slack. Shown in Fig. 5 (top) is a section of the energy surface when the saddles corotate ($\theta_1=\theta_2$). The system is seen to be *unstable* with respect to this motion. Fig. 5 (middle and bottom) shows the strains in the two bars with corotation. The fact that the strain dependency on rotation has zero slope at the equilibrium point indicates the necessity for a finite deformation analysis, which shows that both bars release their prestrain when the saddles corotate. Due to the concave potential energy profile, this unloading will occur spontaneously. The only restraint to this instability will come from friction between the main pin and the saddle (or any hard rotation stops that may exist in the system). It should also be noted that if either the top or the bottom saddle is held in a stop and the other saddle is left free, then this configuration is stable; see Figs. 6 and 7.

Configuration 2: Alternative Configuration

As an alternative to the as installed configuration, we also consider a configuration where the attachment points of the bars are placed between the main pins, as shown in Fig. 1 (right). Fig. 8 shows the potential energy of the system with respect to the saddle rotations. When the saddles counter-rotate the energy grows and the system is seen to be stable against this type of motion. A section cut of the energy surface for $\theta_1=-\theta_2$ is shown in Fig. 9 (top). This behavior is similar to Configuration 1. Also shown in Fig. 9 (middle and bottom) are the strains in the bars along this path and they show similar behavior to Configuration 1. With excessive rotations individual bars can go slack as before. Shown in Fig. 10 (top) is a section of the energy surface when the saddles corotate ($\theta_1=\theta_2$). The system is seen now to be *stable* with respect to this motion in contradistinction to Configuration 1.

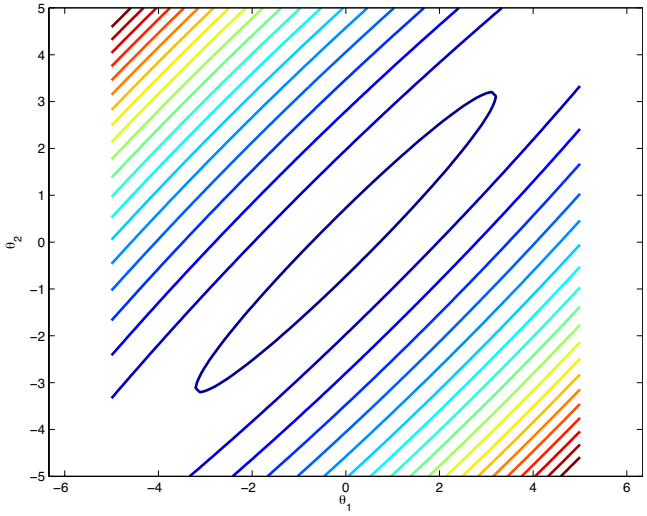

Fig. 8. Potential energy contour lines as a function of the saddle rotations for Configuration 2. An equilibrium is visible at zero total rotation and it possesses a stable bowl-like structure. Contour values increase to the upper left and lower right.

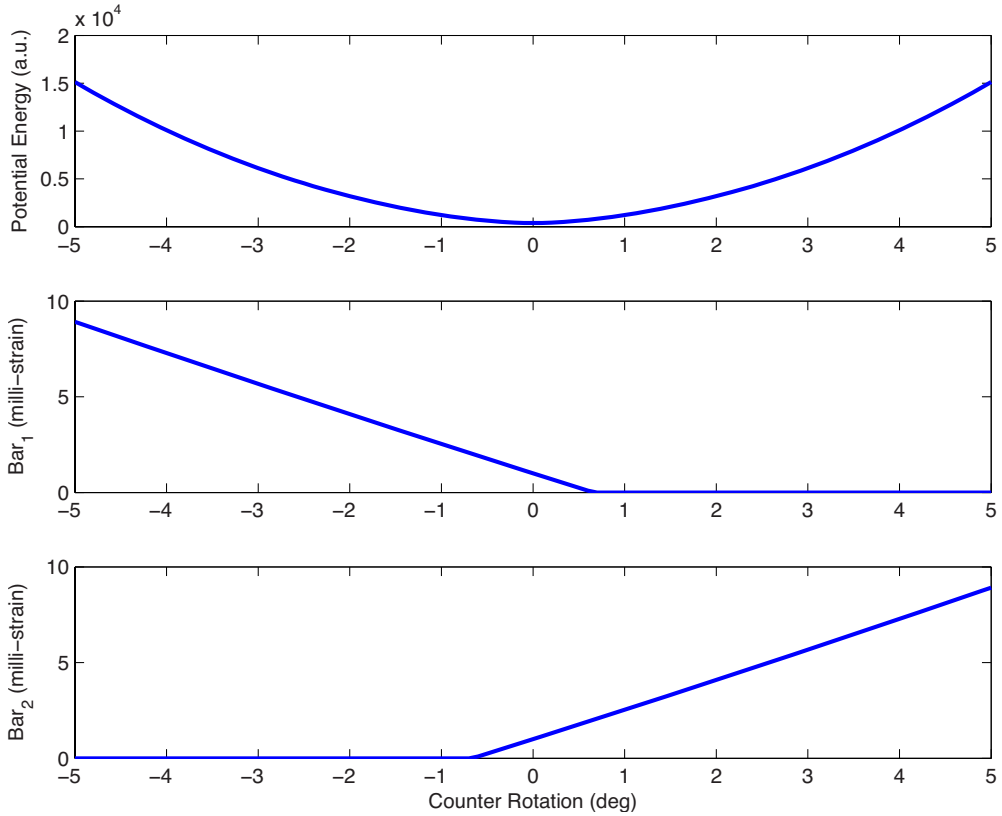

Fig. 9. Configuration 2 behavior for counter-rotating saddles ($\theta_1 = -\theta_2$). (Top) Potential energy is seen to be stable. (Middle) Strain in Bar 1. (Bottom) Strain in Bar 2. Strains are zero when the bars go slack.

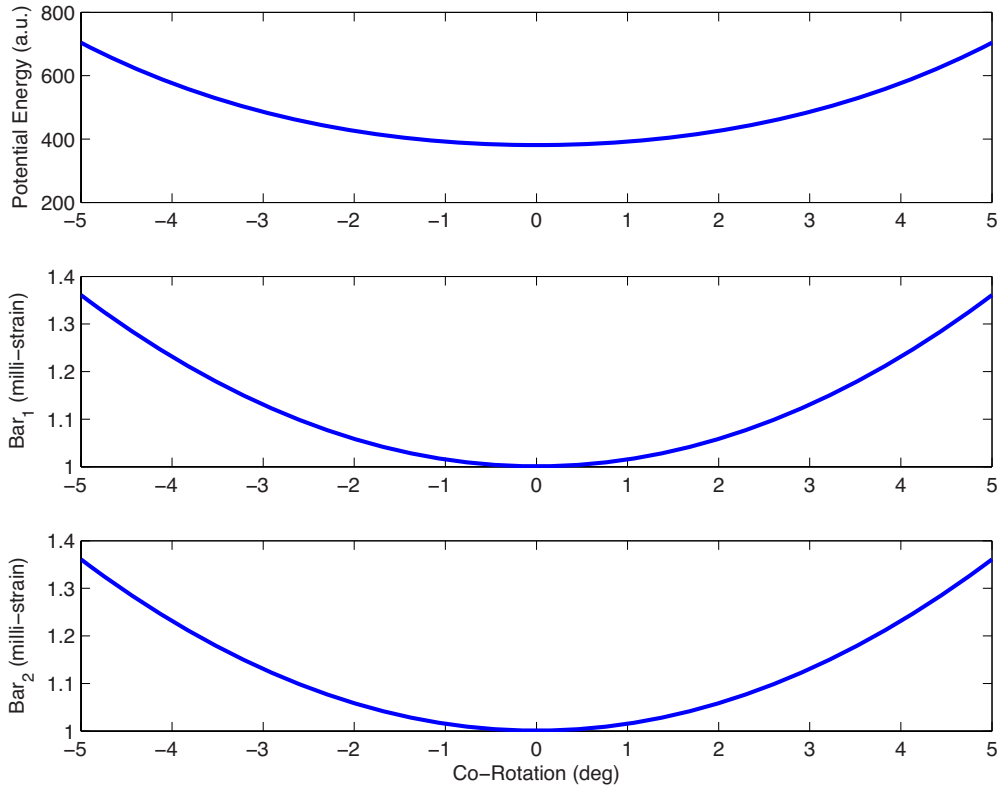

Fig. 10. Configuration 2 behavior for corotating saddles ($\theta_1 = \theta_2$). (Top) Potential energy is seen to be stable. (Middle) Strain in Bar 1. (Bottom) Strain in Bar 2.

As shown in Fig. 10 (middle and bottom), both bars pick up strain when the saddles corotate and do not unload. Due to the convex potential energy profile, this mode of deformation will not occur spontaneously and thus the system is self-centering.

Conclusion

A simple and straightforward analysis shows that the as designed repair system is inherently unstable and that a simple reconfiguration eliminates this problem. A broader question, which requires precise access to the system's geometry and properties, is whether or not this instability led to the repair system's failure. Notwithstanding, it is clear that such instability is not helpful and can in the mind's eye easily lead to many deleterious effects such as repeated large system motions, transverse loads on truss members, etc.

Acknowledgments

S.G. gratefully acknowledges M. Zahr for his assistance in the preparation of the drawings of the saddle repair system.

References

Fung, Y. C. (1965). *Foundations of solid mechanics*, Prentice-Hall, Englewood Cliffs, N.J.

Timoshenko, S., and Gere, J. (1961). *Theory of elastic stability*, McGraw-Hill, New York.